Supporting Information

Tuning hexagonal $NaYbF_4$ nanocrystals down to sub-10 nm for enhanced photon upconversion

Ruikai Shi,[a] Xincan Ling,[a] Xiaona Li,[a] Lu Zhang,[a] Min Lu,[a] Xiaoji Xie,*[a] Ling Huang*[a] and Wei Huang[ab]

[a]*Key Laboratory of Flexible Electronics (KLOFE) & Institute of Advanced Materials (IAM), Jiangsu National Synergetic Innovation Center for Advanced Materials (SICAM), Nanjing Tech University (NanjingTech), 30 South Puzhu Road, Nanjing 211816, P.R. China*

[b]*Key Laboratory for Organic Electronics and Information Displays & Institute of Advanced Materials (IAM), Jiangsu National Synergetic Innovation Center for Advanced Materials (SICAM), Nanjing University of Posts & Telecommunications, 9 Wenyuan Road, Nanjing 210023, China.*

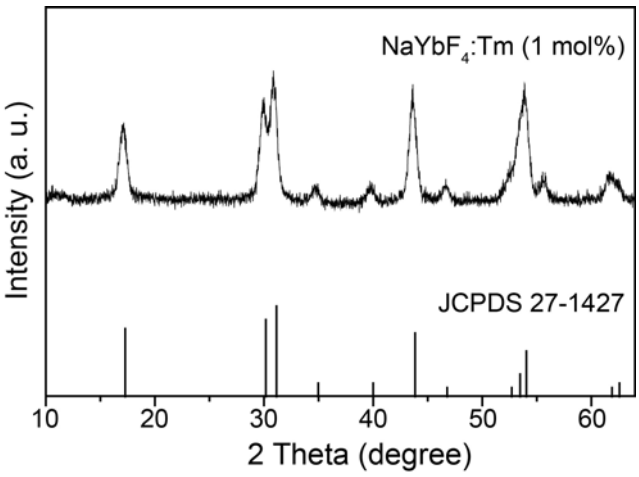

Fig. S1 XRD pattern of the as-synthesized $NaYbF_4$:Tm (1 mol%) nanocrystals. The diffraction pattern at the bottom is the literature reference for hexagonal $NaYbF_4$ crystal (Joint Committee on Powder Diffraction Standards file number 27-1427). The XRD pattern indicates that the as-synthesized $NaYbF_4$ nanocrystals are pure hexagonal phase. Note that the peak at ~55° can be attributed to the diffraction of (102), which was observed in both literature reports of hexagonal $NaYbF_4$ nanocrystals and other hexagonal $NaLnF_4$ (Ln = Y, Er, Tm, and Lu) crystals.

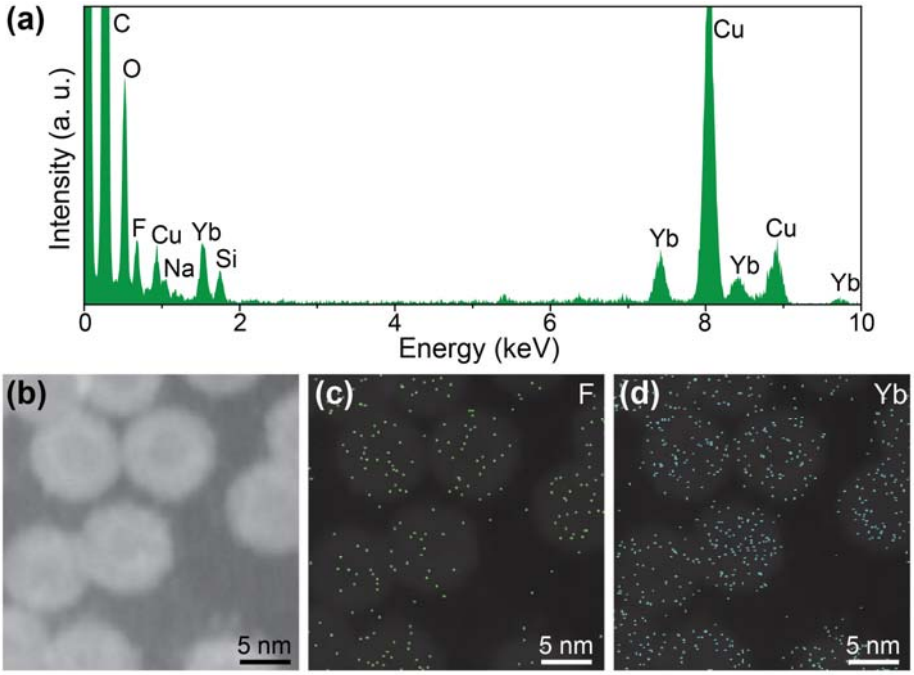

Fig. S2 (a) The energy dispersive X-ray spectrum of the as-synthesized $NaYbF_4$:Tm (1 mol%) nanocrystals, revealing the presence of Na, Yb and F. (b) STEM image of the $NaYbF_4$:Tm (1 mol%) nanocrystals. (c-d) The corresponding F and Yb distributions of the nanocrystals shown in (b). Note that the element maps, in (c) and (d), are overlapped with the STEM image for comparison.

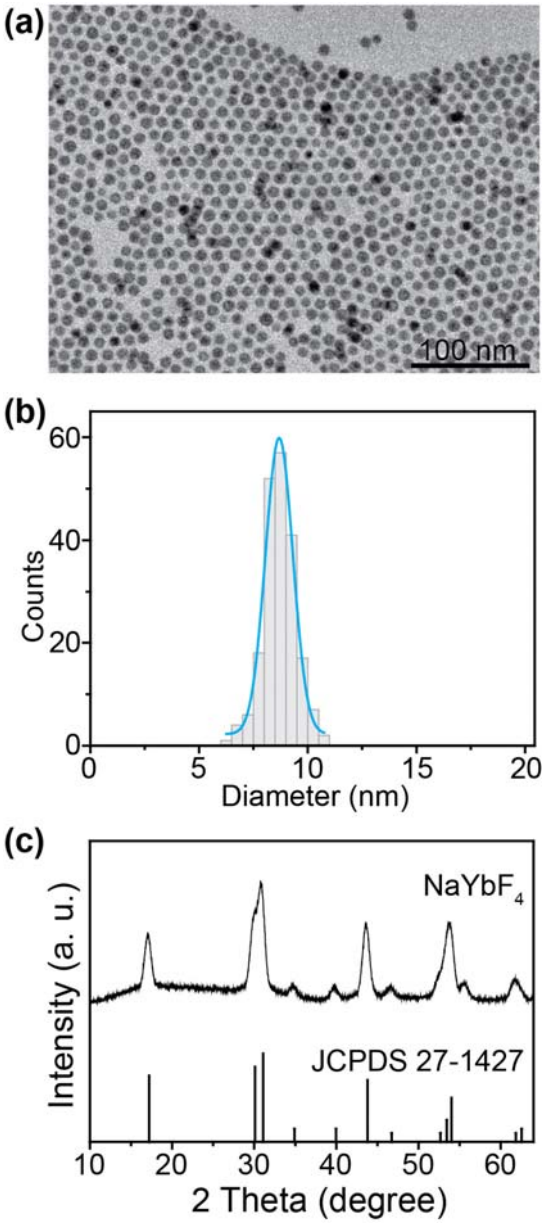

Fig. S3 TEM image (a), corresponding size distribution (b) and XRD pattern (c) of the as-synthesized $NaYbF_4$ nanocrystals without doping. The diffraction pattern at the bottom of (c) is the literature reference for hexagonal $NaYbF_4$ crystal (JCPSD 27-1427).

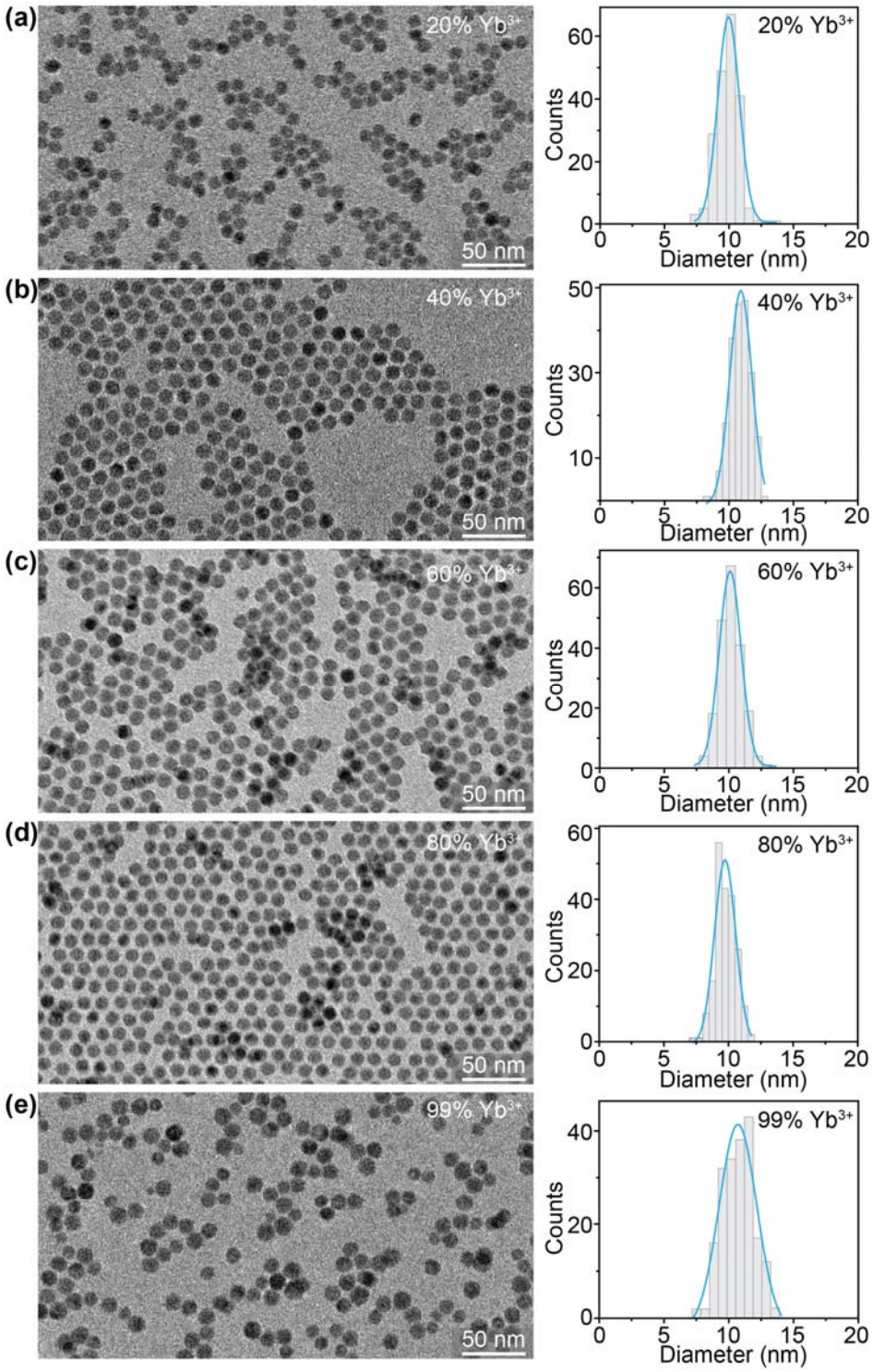

Fig. S4 TEM images and corresponding size distributions of $NaYbF_4$:Y/Tm nanocrystals containing varied amounts of Yb^{3+} ions. The doping concentration of Tm^{3+} ions is 1 mol% and the concentrations of Yb^{3+} ions for (a-e) are 20, 40, 60, 80, and 99 mol%, respectively.

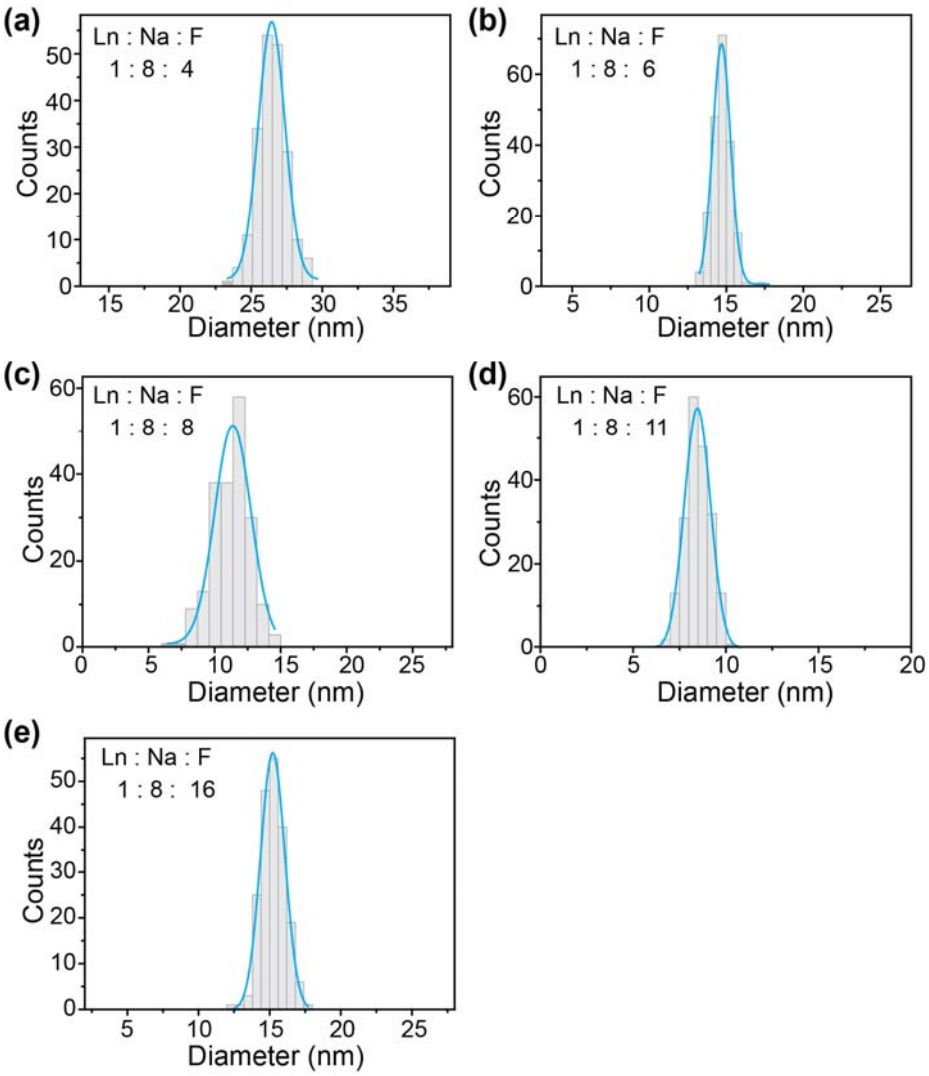

Fig. S5 The size distributions of $NaYbF_4$:Tm (1 mol%) upconversion nanocrystals obtained at varied molar ratios of lanthanide ions (Ln), sodium oleate (Na) and NH_4F (F). The corresponding TEM images are shown in Fig. 2.

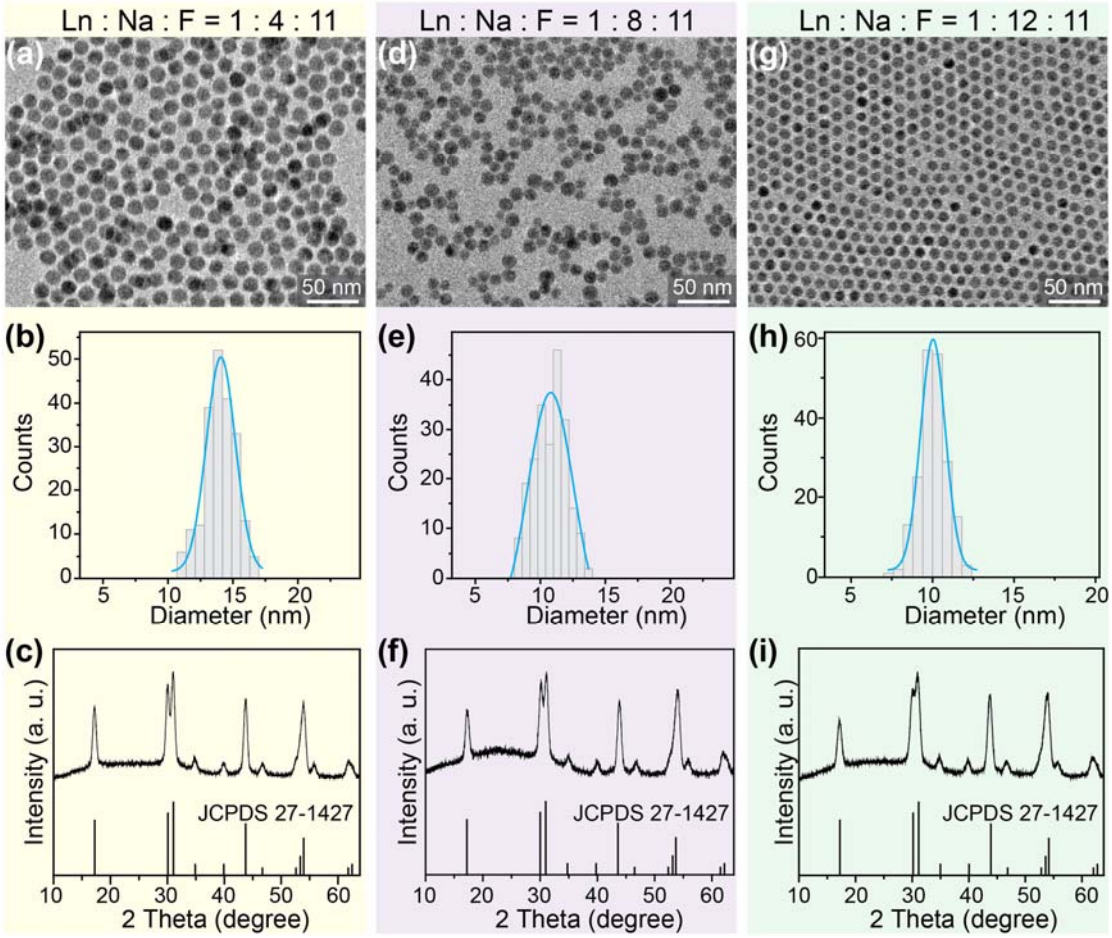

Fig. S6 TEM images, corresponding size distributions and XRD patterns of the $NaYbF_4$:Tm (1 mol%) nanocrystals synthesized at varied molar ratios of lanthanide ions (Ln), sodium oleate (Na) and NH_4F (F). (a-c) Ln : Na : F = 1 : 4 : 11, (d-f) Ln : Na : F = 1 : 8 : 11, and (g-i) Ln : Na : F = 1 : 12 : 11. The diffraction patterns at the bottom of (c), (f) and (i) are the literature reference for hexagonal $NaYbF_4$ crystal (Joint Committee on Powder Diffraction Standards file number 27-1427).

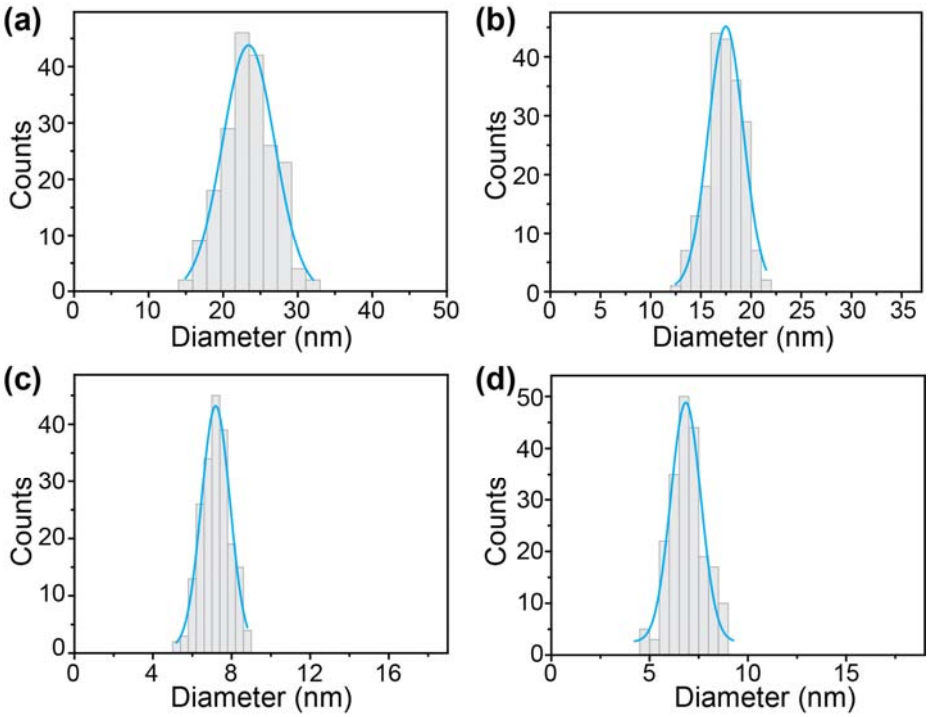

Fig. S7 The size distributions of $NaYbF_4$:Tm (1 mol%) upconversion nanocrystals obtained at varied amounts of oleic acid. The volume ratios of oleic acid and octadecene for (a-d) are 3 : 17, 6 : 14, 14 : 6, and 17 : 3, respectively. The corresponding TEM images are shown in Fig. 3.

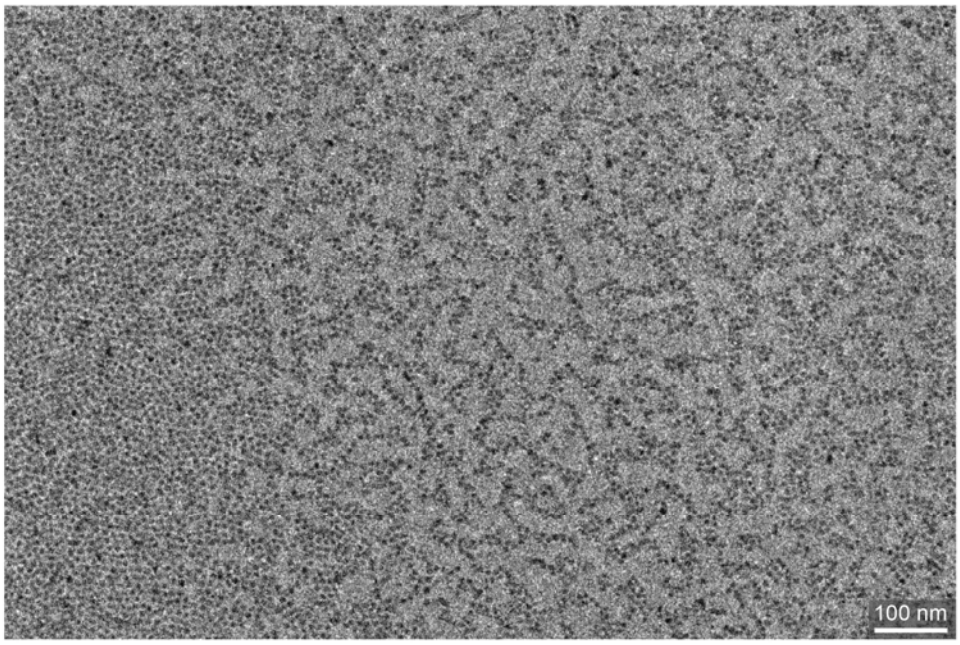

Fig. S8 Large scale TEM image of $NaYbF_4$:Tm (1 mol%) upconversion nanocrystals, ~7 nm, obtained in the presence of 17 mL oleic acid and 3 mL octadecene.

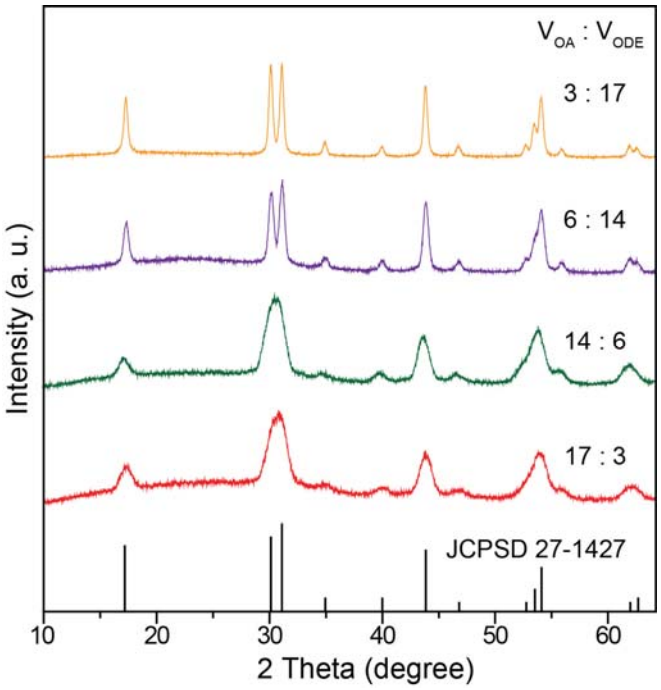

Fig. S9 XRD patterns of $NaYbF_4$:Tm (1 mol%) upconversion nanocrystals obtained at varied amounts of oleic acid. The volume ratios of oleic acid (V_{OA}) and octadecene (V_{ODE}) are 3 : 17, 6 : 14, 14 : 6, and 17 : 3, respectively. The diffraction pattern at the bottom is the literature reference for hexagonal $NaYbF_4$ crystal (JCPSD 27-1427).

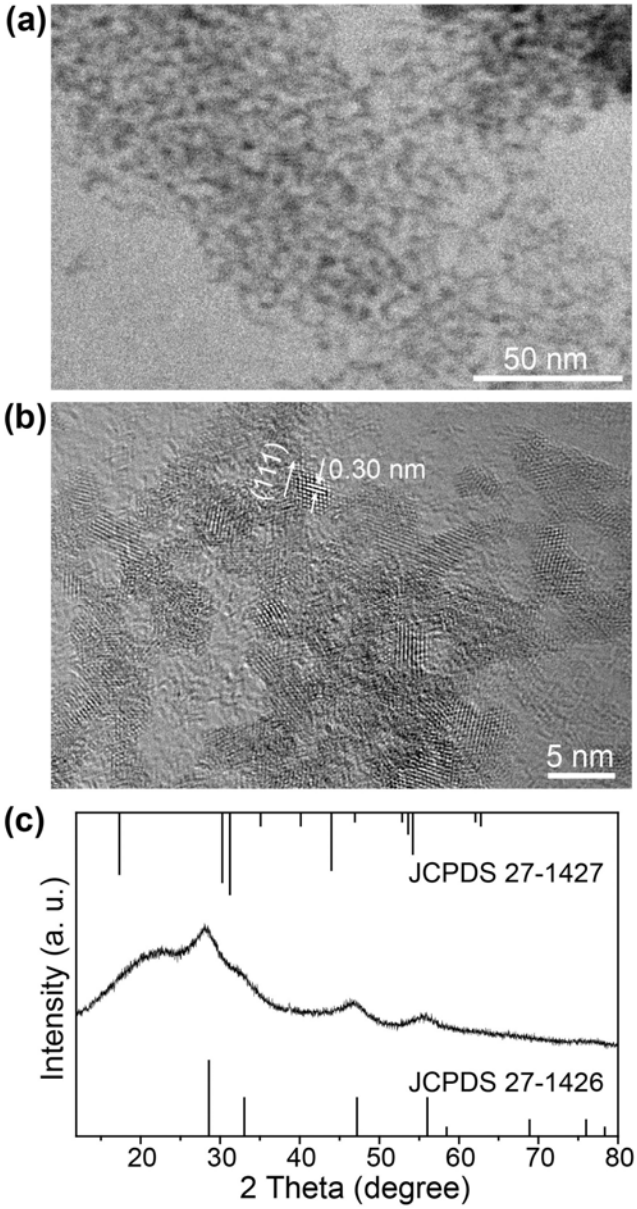

Fig. S10 TEM image (a), HRTEM image (b) and corresponding XRD pattern (c) of the nanocrystals obtained after reacting at 160 ^{o}C for 1 h. The diffraction patterns at the top and bottom are the literature references for hexagonal $NaYbF_4$ crystal (JCPSD 27-1427) and cubic $Na_5Yb_9F_{32}$ crystal (JCPDS 27-1426), respectively.

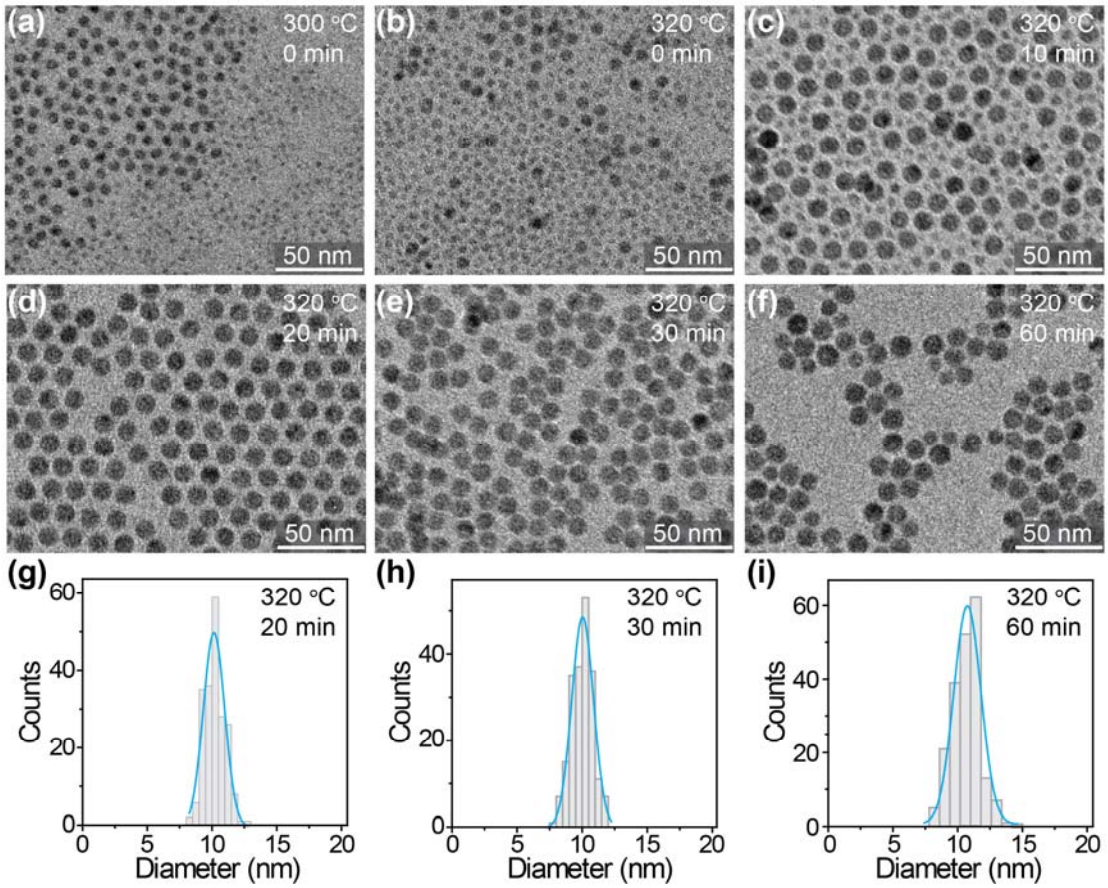

Fig. S11 (a-f) TEM images of products extracted from the reaction mixture at different temperatures and times. (g-i) Corresponding size distributions of the nanocrystals shown in (d-f), respectively.

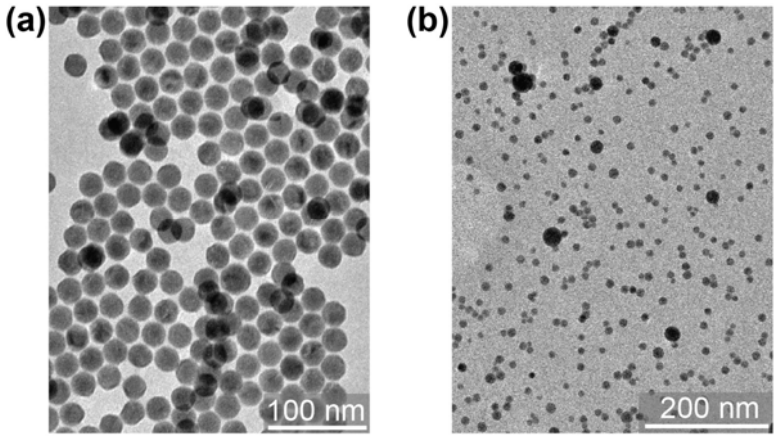

Fig. S12 TEM images of $NaYbF_4$ nanocrystals obtained without heating at 160 ^{o}C for 1 h.

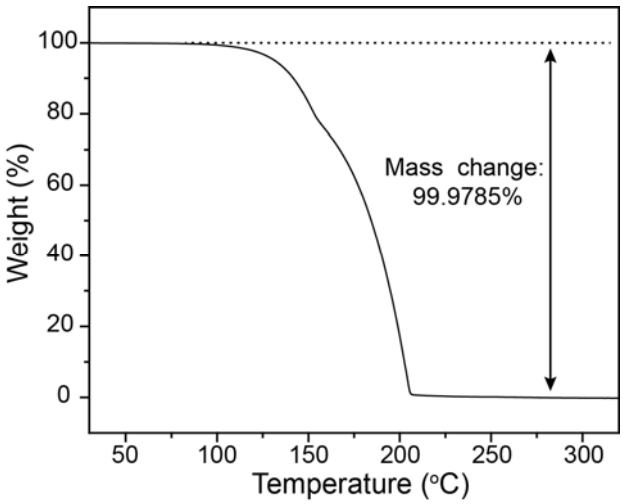

Fig. S13 Thermogravimetric analysis curve of NH_4F. The curve indicates that NH_4F starts to decompose at ~100 °C and can be complete decomposed under continuous heating.

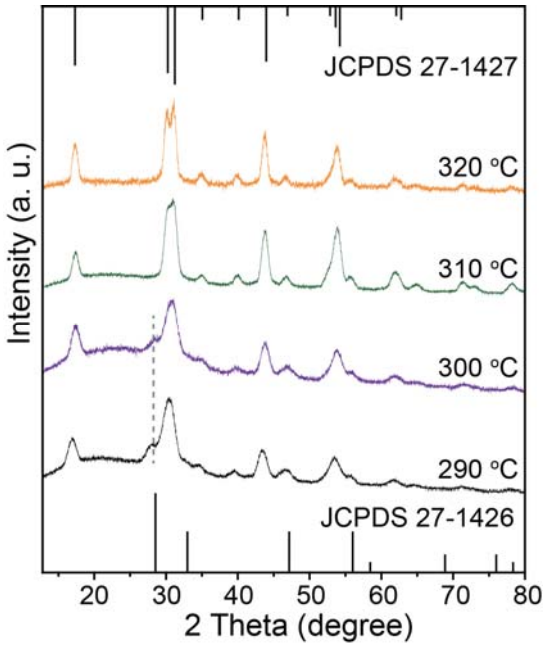

Fig. S14 XRD patterns of $NaYbF_4$:Tm (1 mol%) nanocrystals obtained after reacting at different temperatures for 30 min. The diffraction patterns at the top and bottom are the literature references for hexagonal $NaYbF_4$ crystal (JCPSD 27-1427) and cubic $Na_5Yb_9F_{32}$ crystal (JCPDS 27-1426), respectively. After reacting at 290 and 300 °C for 30 min, there still exist cubic phase crystals as indicated by the dashed line.

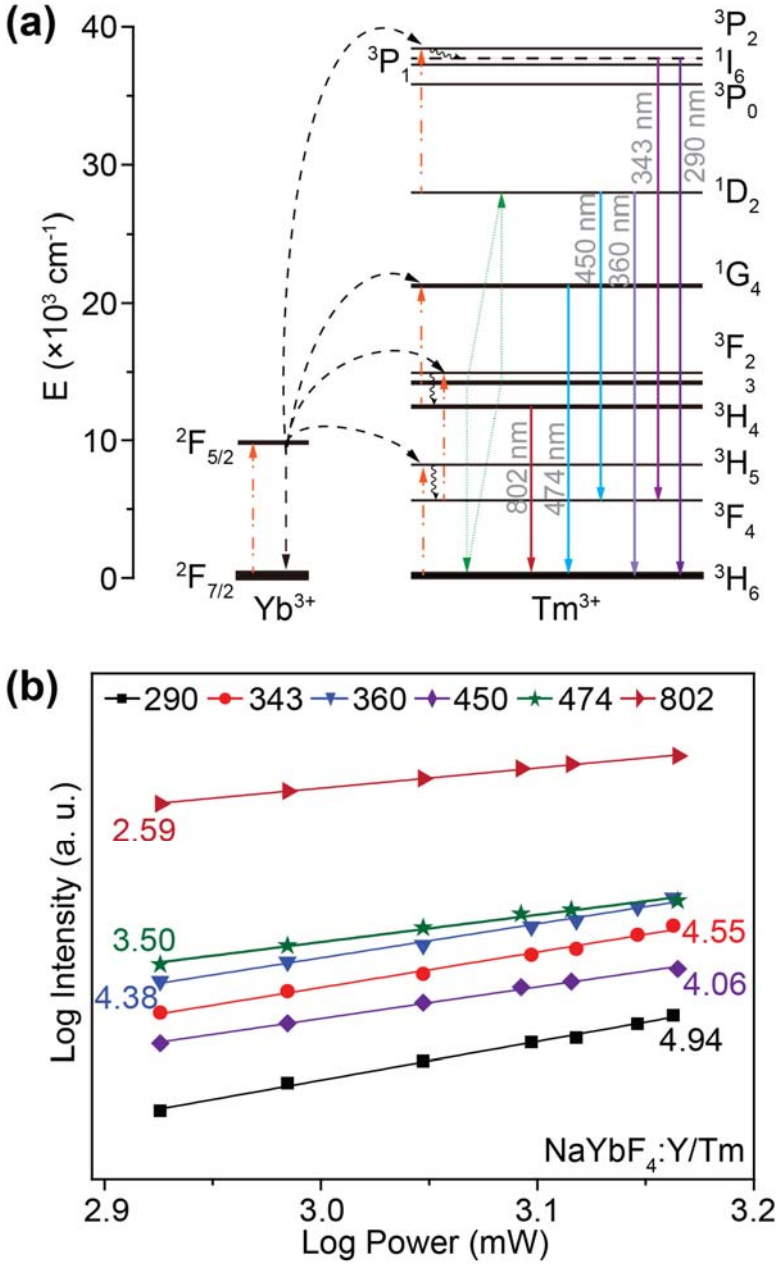

Fig. S15 (a) Proposed upconversion processes of $NaYbF_4$:Tm nanocrystals. The dashed-dotted, dashed, dotted, wavy, and solid arrows represent photon excitation, energy transfer, cross relaxation, multiphonon relaxation, and emission processes, respectively. (b) Log-log plots of upconversion emission intensity against the excitation power for $NaYbF_4$:Y/Tm (79/1 mol%) nanocrystals.

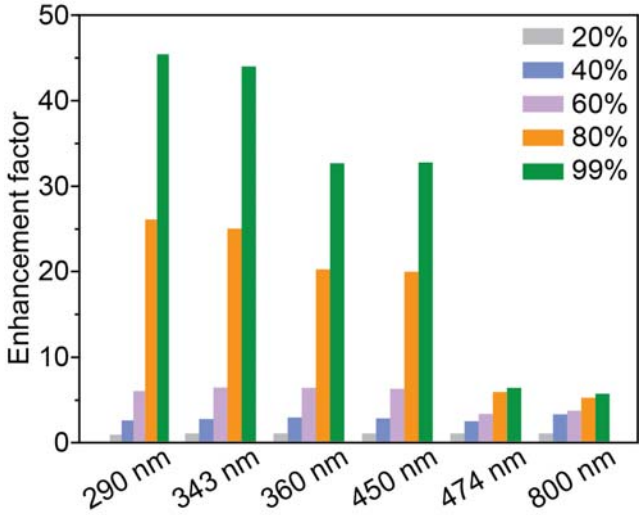

Fig. S16 Comparison of upconversion luminescence intensity of $NaYbF_4$:Y/Tm nanocrystals containing varied amounts of Yb^{3+} (20-99 mo%) at different emission bands. To vary the doping concentration of Yb^{3+}, optically inert Y^{3+} ions were used to replace Yb^{3+} ions and the TEM images of the nanocrystals were shown in Fig. S4. The enhancement factors were obtained by comparing the upconversion emission intensity of the obtained nanocrystals with that of $NaYbF_4$:Y/Tm (79/1 mol%) nanocrystals, with 20 mol% Yb^{3+}.

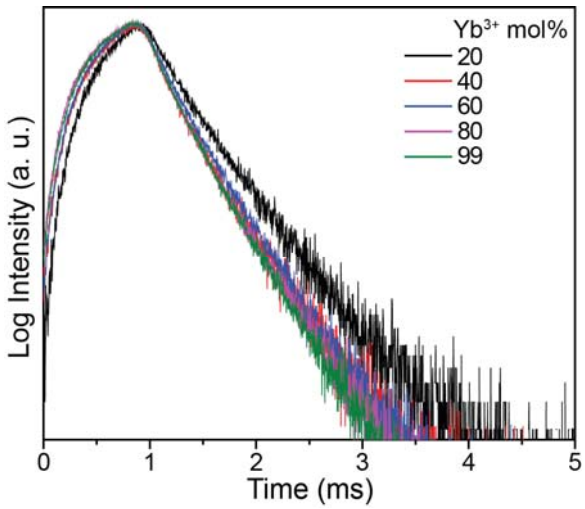

Fig. S17 Upconversion luminescence decay curves (Tm^{3+}: $^1G_4$ to $^3H_6$) of $NaYbF_4$:Y/Tm nanocrystals containing varied amounts of Yb^{3+} (20-99 mo%) under 980 nm laser excitation.

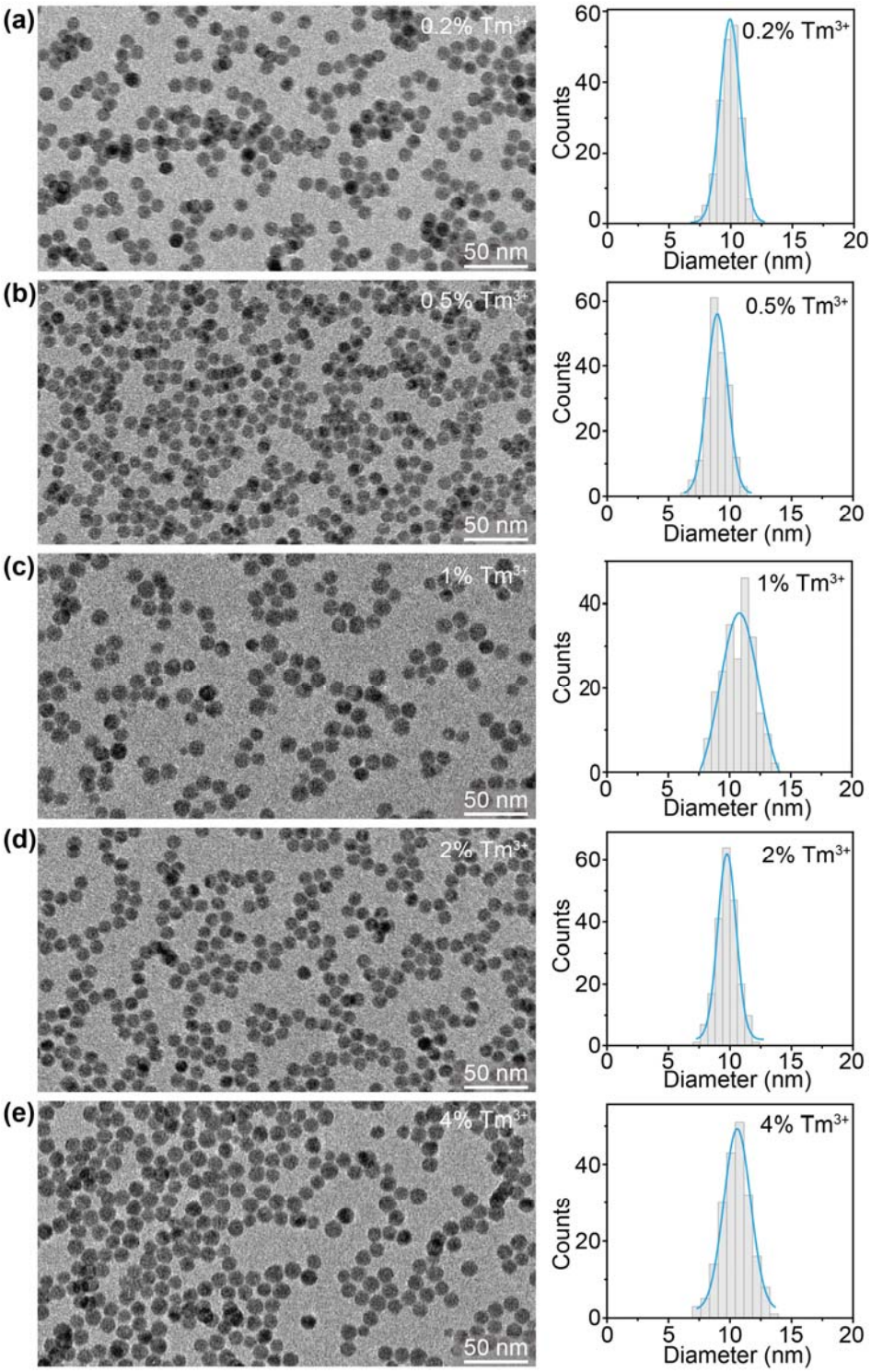

Fig. S18 TEM images and corresponding size distributions of $NaYbF_4$:Tm nanocrystals doped with varied amounts of Tm^{3+} ions. The doping concentrations of Tm^{3+} ions for (a-e) are 0.2, 0.5, 1, 2, and 4 mol%, respectively.

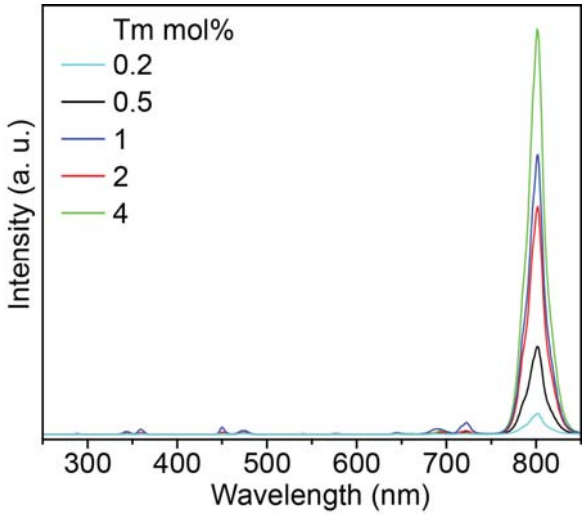

Fig. S19 Upconversion luminescence spectra of $NaYbF_4$:Tm nanocrystals doped with varied Tm^{3+} under 980 nm laser excitation. For spectrum measurement, the nanocrystals were dispersed in cyclohexane with the same mass concentration.

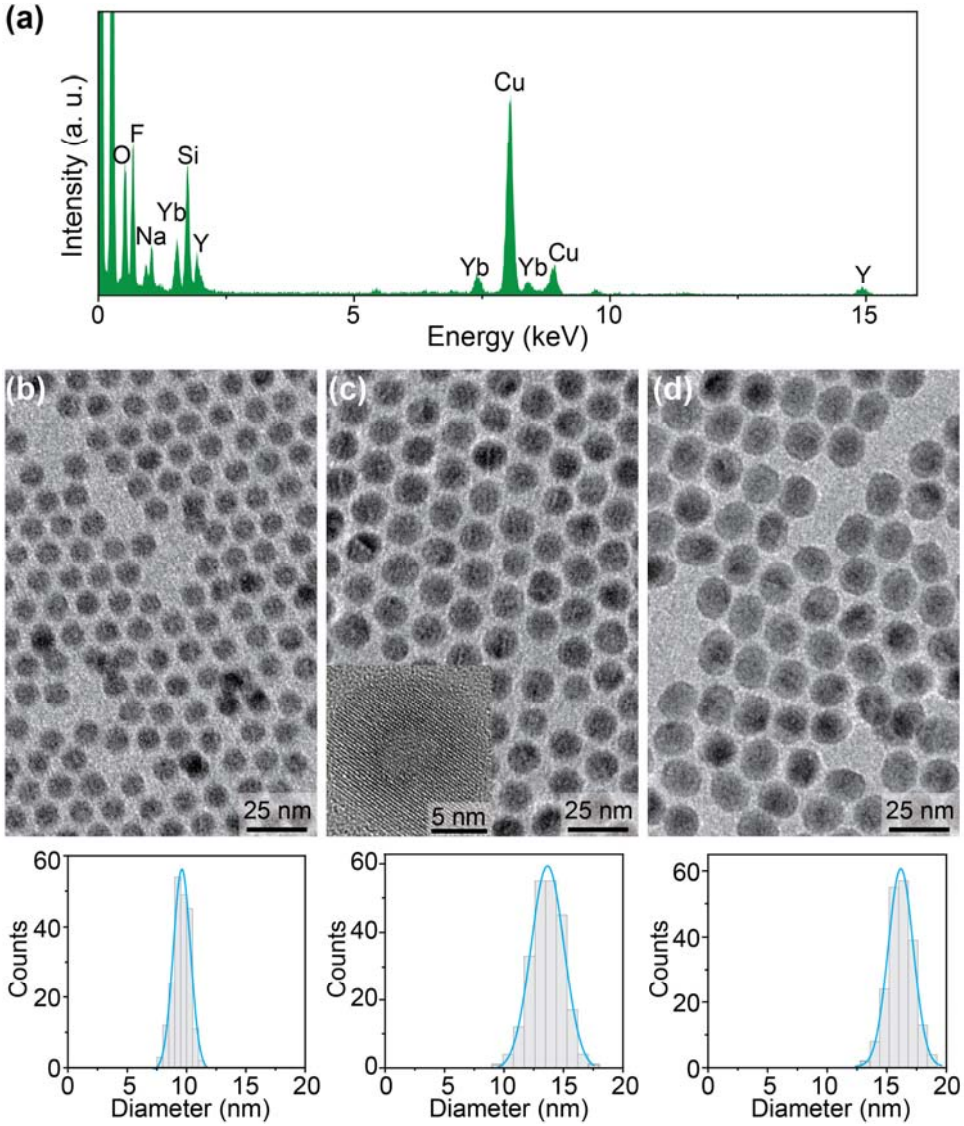

Fig. S20 (a) The energy dispersive X-ray spectrum of the as-synthesized $NaYbF_4$:Tm@$NaYF_4$ core-shell nanocrystals, revealing the presence of Y, Yb, F and Na. (b) TEM image and corresponding size distribution of $NaYbF_4$:Tm (1 mol%) core nanocrystals. (c-d) TEM images and corresponding size distributions of the $NaYbF_4$:Tm (1 mol%) nanocrystals, shown in (b), after coating a $NaYF_4$ shell with different thickness. The inset in (c) is the HRTEM image of a core-shell nanocrystal indicating single-crystalline structure.

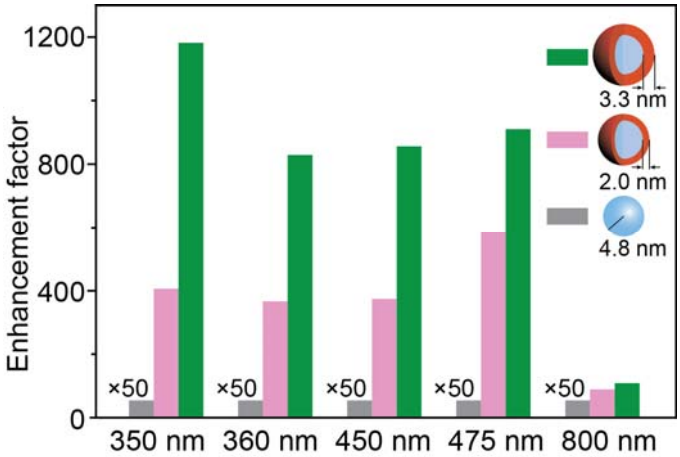

Fig. S21 Comparison of upconversion luminescence intensity of $NaYbF_4$:Tm (1 mol%) core and $NaYbF_4$:Tm (1 mol%)@$NaYF_4$ core-shell nanocrystals with different shell thicknesses at different emission bands. The TEM images and corresponding upconversion emission spectra of the nanocrystals were shown in Fig. S20 and Fig. 6, respectively. The enhancement factors were obtained by comparing the upconversion emission intensity of the obtained nanocrystals with that of the $NaYbF_4$:Tm (1 mol%) core nanocrystals.

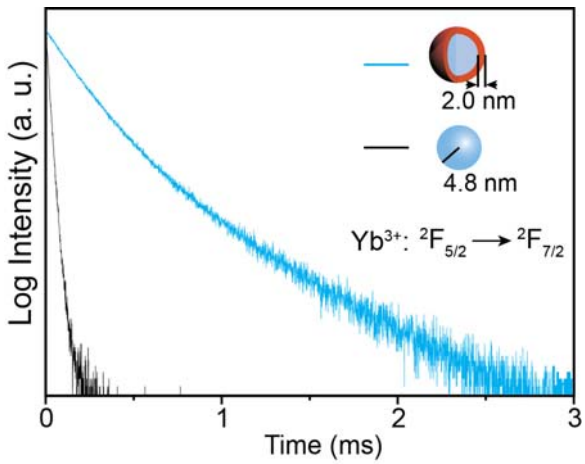

Fig. S22 Luminescence decay curves (Yb^{3+}: $^2F_{5/2}$ to $^2F_{7/2}$) of $NaYbF_4$:Tm (1 mol%) core and $NaYbF_4$:Tm (1 mol%)@$NaYF_4$ core-shell nanocrystals under 980 nm laser excitation.

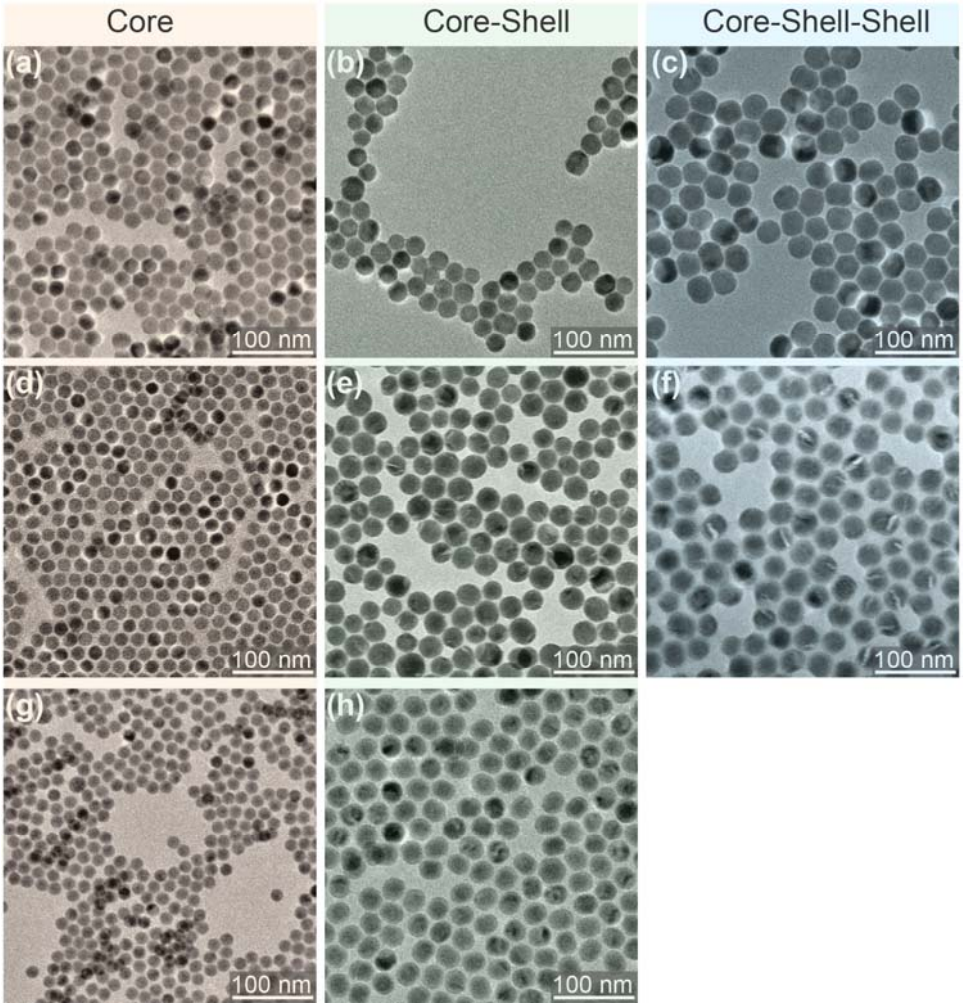

Fig. S23 (a-c) TEM images of the $NaYF_4$ core, $NaYF_4$@$NaYbF_4$:Tm core-shell, and $NaYF_4$@$NaYbF_4$:Tm@$NaYF_4$ core-shell-shell nanocrystals. The thickness of $NaYbF_4$:Tm shell layer is ~1.9 nm. (d-f) TEM images of the $NaYF_4$ core, $NaYF_4$@$NaYbF_4$:Tm core-shell, and $NaYF_4$@$NaYbF_4$:Tm@$NaYF_4$ core-shell-shell nanocrystals. The thickness of $NaYbF_4$:Tm shell layer is ~3.6 nm. (g-h) TEM images of the $NaYbF_4$:Tm core, and $NaYbF_4$:Tm@$NaYF_4$ core-shell nanocrystals.

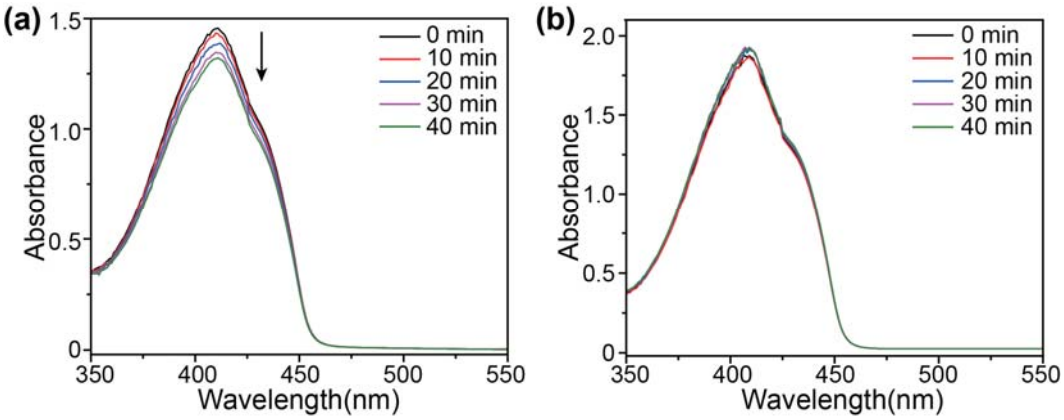

Fig. S24 (a-b) Absorbance spectra of 1,3-diphenylisobenzofuran (DPBF, 2 mg/mL) solution in the presence (a) and absence (b) of ~10 nm $NaYbF_4$:Tm (1 mol%) nanocrystals after irradiation of 980 nm laser (~3 W) for different time intervals. DPBF was used as an indicator for reactive oxygen species. In the presence of $NaYbF_4$:Tm nanocrystals, reactive oxygen species were observed under 980 nm laser irradiation as indicated by the decrease of DPBF absorption at ~410 nm. In contrast, in the absence of $NaYbF_4$:Tm nanocrystals, no obvious decrease of DPBF absorption was observed. These results indicate that $NaYbF_4$:Tm nanocrystals can work as photosensitizers under near infrared light excitation.